

# Comparative Analysis of Peculiar Type Ia 1991bg-like Supernovae Spectra

Brandon A. Doull and E. Baron

*Homer L. Dodge Department of Physics and Astronomy,  
The University of Oklahoma,  
Norman, Oklahoma*

doull@nhn.ou.edu

## ABSTRACT

Spectroscopic analyses of Type Ia supernovae have shown there exist four spectroscopic groups—cools, broad line, shallow silicon, and core normal—defined by the widths of the Si II features  $\lambda 5972$  and  $\lambda 6355$ . 1991bg-likes are classified as “cools”. Cools are dim, undergo a rapid decline in luminosity, and produce significantly less  $^{56}\text{Ni}$  than normal Type Ia supernovae. They also have an unusually deep and wide trough in their spectra around  $4200 \text{ \AA}$  and a relatively strong Si II absorption attributed to  $\lambda 5972$ . We examine the spectra of supernova (SN) 1991bg and the cools SN 1997cn, SN 1999by, and SN 2005bl using the highly parameterized synthetic spectrum code **SYNOW**, and find general agreement with similar spectroscopic studies. Our analysis reveals that this group of supernovae is fairly homogeneous, with many of the blue spectral features well fit by Fe II. The nature of the spectroscopic commonalities and the variations in the class are discussed. Finally, we examine intermediates such as SN 2004eo and discuss the spectroscopic subgroup distribution of Type Ia supernovae.

*Subject headings:* supernovae: individual (1991bg, 1997cn, 1999by, 2005bl)

## 1. Introduction

Type Ia supernovae (hereafter SNe Ia) are important objects in the study of nucleosynthesis, stellar evolution, and modern cosmology. It is believed that SNe Ia are thermonuclear explosions of carbon-oxygen white dwarfs which have approached to within about 1% of the Chandrasekhar Mass ( $1.39M_{\odot}$ ) (Hillebrandt & Niemeyer 2000; Höflich et al. 2010). In cosmology, SNe Ia were suggested early on (Baade 1938) to be useful as standard candles for making accurate distance measurements in the determination of cosmological parameters, because of both their significant homogeneity in absolute bolometric magnitude and large apparent brightness. With modern supernova surveys such as the Supernova Cosmology Project, ESSENCE Supernova Survey, Nearby Supernova Factory, Palomar Transient Factory, Supernova Legacy Survey, and the Large Synoptic Survey Telescope, accurate measurements of these parameters based on SNe Ia at varying redshifts

have been and continue to be made (Perlmutter et al. 1999; Krisciunas 2008; Copin et al. 2006; Law et al. 2009; Conley et al. 2011; LSST Science Collaborations et al. 2009). It has even been possible to measure the rate of expansion of the universe and put limits on cosmological models (Riess et al. 1998; Goobar et al. 2000; Wood-Vasey et al. 2007; Riess et al. 2009; Hicken et al. 2009; Chuang & Wang 2011; Parkinson et al. 2010). It is because of this important role SNe Ia play that a deep understanding of their properties, variations, and evolution is vital.

In our study we have narrowed our focus to the “cool” spectroscopic subgroup, epitomized by SN 1991bg which occurred in NGC 4374, and so-called “intermediates” which could potentially bridge the gap between the four spectroscopic subgroups. We used the highly-parameterized synthetic spectrum code **SYNOW** to model the spectra of several cool SNe Ia. To better understand the **SYNOW** code and its use see Branch et al. (2007, 2003, 2002), and for more in depth technical details see Fisher (2000). The spectra range from a few days before  $B$  maximum to as late as one month post  $B$  maximum in the optical spectra with wavelengths from the Ca II H&K feature in the blue to the Ca II infrared triplet. The spectra have been corrected for redshift of their host galaxies and normalized to remove the slope of the continuum, as we are primarily interested in spectral features for making line identifications. This normalization, described in Jeffery et al. (2007), also serves to facilitate the comparisons between different supernovae. Extremely noisy spectra have been smoothed using boxcar smoothing.

In §2 the method of spectroscopic sub-classification is discussed. In §3 the properties, progenitors, and possible explosion mechanisms of 1991bg-likes are reviewed, and in §4 our line identifications are given and compared with similar studies. In §5 we discuss the potential of intermediates to fill in the gaps between the seemingly discrete subgroups.

## 2. Spectroscopic Subgroups

For decades, SNe Ia had been accepted for use as standard candles based on their apparent homogeneity, but in 1991 two very peculiar supernovae, SN 1991bg (Filippenko et al. 1992a; Leibundgut et al. 1993) and SN 1991T (Waagen et al. 1991; Filippenko et al. 1992b) challenged the validity of such use. According to work completed by Li et al. (2001) and recently updated (Li et al. 2010) the peculiarity rate for SNe Ia could be as high as 30%, with rates of 1991bg-likes up to 15%. These observed peculiarities instigated the search for parameters which could be used to find a photometric and spectroscopic standard relation, in order to make SNe Ia standardizable candles.

The first relation was found by Phillips (1993) who used a small sample of well-observed SNe Ia to identify a very strong correlation between peak luminosity and initial decline rates, parameterized by  $\Delta m_{15}$ . The  $\Delta m_{15}$  parameter measures the the decline in brightness of the  $B$  band from maximum until 15 days after maximum. The Phillips relation indicates brighter objects will have slower decline rates than dim objects which decline rapidly. An analogous spectroscopic

relation was suggested by Nugent et al. (1995). Nugent’s spectral relation measures the ratio of the strength of the Si II features  $\lambda 5972$  and  $\lambda 6355$ , denoted by  $\mathcal{R}(\text{Si II})$ . The standard relations, both photometric and spectroscopic, are due in large part to temperature differences caused by the amount of radioactive  $^{56}\text{Ni}$  synthesized during the explosion.

Single parameter modeling of SNe Ia is indeed useful, but in cases of extremely peculiar SNe, such as SN 1991bg and SN 1991T, other means of accurate and efficient sub-classification are necessary. Several such classification schemes exist. One scheme proposed by Benetti et al. (2005) is based on the evolution of Si II  $\lambda 6355$  line velocity, while another, proposed by Branch et al. (2006) uses the pseudo-equivalent widths of the Si II lines  $\lambda 5972$  and  $\lambda 6355$ .

By measuring the velocity of Si II  $\lambda 6355$  10 days past  $B$  max as well as the evolution of the velocity of this feature Benetti et al. (2005) found not only a spread in velocities between different SNe Ia, but also a distribution in velocity gradients. Plotting these gradients reveals three groups of SNe Ia which Benetti et al. (2005) labels as faint (FAINT), high temporal velocity gradient (HVG), and low temporal velocity gradient (LVG) (Benetti 2005; Benetti et al. 2005). The FAINT subgroup corresponds to subluminous 1991bg-like events with low expansion velocities and a large velocity gradient. The HVG group contains normal SNe Ia with high expansion velocities and a high velocity gradient. Finally, the LVG group contains both normal SNe Ia as well as the brightest SNe Ia. This group has, on average, lower expansion velocities than the HVG group and a low velocity gradient.

In the scheme of Branch et al. (2006), the pseudo-equivalent widths of Si II lines  $\lambda 5972$  and  $\lambda 6355$  are measured and plotted (since emission lines are present in the spectra, these are not true equivalent widths but rather widths whose limits of integration have been chosen by eye). We followed the example of Branch et al. (2006) and plotted the width of the  $\lambda 5972$  feature vs. the width of the  $\lambda 6355$  feature for a sample of SNe Ia. This plot can be seen in Figure 1 and shows a cluster of core-normal (CN) SNe Ia with three discrete branches representing the peculiar spectroscopic subgroups of cool (CL), broad-line (BL), and shallow silicon (SS). The CLs correspond to Benetti’s FAINT, BL tend to fall into the HVG group, and the LVG contains both CN and SS.

In this method, each of the spectroscopic subgroups have their own differing properties and are named accordingly. CNs are the most common and well studied SNe Ia and are found in the region of highest density in the pseudo-equivalent width (WW) plot of Figure 1. SN 1994D is an example of a CN SNe Ia. BL SNe Ia have Si II lines whose absorptions are broader and deeper than CNs and thus form the lower right branch of the WW plot in Figure 1. The SNe Ia in the BL subgroup generally have the same ions that are present in CN, but with higher velocities. One such BL SNe Ia is SN 2002bo (Branch et al. 2006). The SS SNe fall to the lower left of the plot in Figure 1 because of their smaller values for Si II widths, but otherwise they have normal SNe Ia spectra. (The CLs will be discussed in depth in §3.) Although the plot indicates there are separate spectroscopic subgroups the borders are not defined by a clear demarcation; instead some overlap exists. We call the SNe Ia which lie between different subgroups “intermediates”.

### 3. Cool Type Ia Supernovae

Spectroscopically peculiar SNe Ia which fall into the cool subgroup share several distinct characteristics. Most notably, cools are subluminous. SN 1991bg had  $V$  and  $B$  maxima which were 1.6 and 2.5 magnitudes, respectively, lower than ordinary SNe Ia (Filippenko et al. 1992a). The CLs also have much faster declines from peak luminosity than do CNs. Typically, CLs have  $\Delta m_{15}(B) \approx 1.9$ , while CNs have  $\Delta m_{15}(B) \approx 1.1$  (Taubenberger et al. 2008). Light curves of SN 1991bg and SN 1994D can be found in Figure 2 showing appropriate  $\Delta m_{15}(B)$  values. It has been established that  $^{56}\text{Ni}$  production is fundamental to determining SNe Ia peak luminosities (Arnett et al. 1985; Branch & Tammann 1992). Analyses of SN 1991bg and other CLs have indicated  $^{56}\text{Ni}$  production of only about 1/6 the amount synthesized during a normal event (Mazzali et al. 1997). Spectroscopically, we see primarily that CLs have an unusually deep and wide absorption trough at around 4200 Å and a very strong Si II  $\lambda 5972$  absorption as shown in Figure 3. The 4200 Å trough is well fit by Ti II which can be explained by its low excitation temperature and the cool nature of these SNe Ia (Filippenko et al. 1992a; Mazzali et al. 1997). Finally, CLs also have a strong and narrow absorption at about 5675 Å usually attributed to Na I D  $\lambda 5893$  (Filippenko et al. 1992a; Garnavich et al. 2004).

#### 3.1. Progenitors

To date, many theories and models have been proposed in attempts to describe the progenitors which lead to SNe Ia, as well as to account for their diversity. Two common scenarios leading to SNe Ia are generally accepted. One scenario is a single degenerate (SD) case proposed by Whelan & Iben (1973) in which a white dwarf (WD) accretes mass until the Chandrasekhar Mass ( $M_{Ch}$ ) is approached, igniting carbon in the core, undergoing thermonuclear instability, and ending with the complete disruption of the WD. A competing scenario proposed by Iben & Tutukov (1984) as well as Webbink (1984) involves two orbiting WDs, where loss of angular momentum due to the emission of gravitational waves leads to an inspiral and eventual merger. The merger of two WDs is referred to as double degenerate (DD). Extensive work has been done to investigate how either a SD scenario or a DD scenario can possibly explain both the homogeneity of SNe Ia while at the same time account for the observed diversity.

SNe Ia appear to be homogeneous because the structure of the WD progenitor and the explosion is determined by nuclear physics (Höflich et al. 2010). That is, the WD is supported by degenerate electron pressure, thermonuclear energy gives the energy production during explosion, and light curves are driven by the decay of synthesized radioactive  $^{56}\text{Ni}$ . According to Höflich (2006), the aspects most important to understanding the diversity are the conditions just prior to explosion and the type of burning mechanism. The basic types of burning can be distinguished as detonation and deflagration. Deflagration occurs with a burning front propagating due to heat transport across the front at a speed of 0.5 – 0.8% the speed of sound (Timmes & Woosley 1992). On the other hand,

in detonations compressional heat ignites carbon and oxygen in front of a shock which propagates supersonically (Höflich 2006).

SD models using delayed detonation—a process where deflagration occurs followed by a transition to detonation—show promise in reproducing observations (Khokhlov 1991). Varying the amount of pre-expansion and burning during the deflagration phase as well as a few other secondary parameters can explain the diversity among SNe Ia in a SD scenario (Höflich et al. 1993; Höflich et al. 2010). Namely, Höflich et al. (2010) decreases the density where transition from deflagration to detonation occurs and in so doing reduces the amount of  $^{56}\text{Ni}$  synthesized thus producing subluminous SNe Ia. It should be noted that the trigger for transition from deflagration to detonation is still not fully understood. When considering the DD scenario recent work using the smoothed particle hydrodynamics code `GADGET3` shows promise in reproducing subluminous SNe Ia akin to 1991bg-like (Pakmor et al. 2011, 2010). They find that this type of merger reproduces the observed results and may be a path to the production of 1991bg-like SNe Ia.

Another method used to investigate SNe Ia progenitors is population synthesis. Through this method, the observed delay time distribution (DTD) of SNe Ia can be used to place limits upon progenitor models and formation scenarios. Taking an observational approach Maoz & Badenes (2010) derive the SN rates and DTD using supernova remnants in the Magellanic Clouds. Maoz & Badenes (2010) find that DTD is proportional to  $t^{-1}$  in agreement with the DD DTD found from population synthesis of DD. Maoz et al. (2011) also confirmed this DTD result using star formation history. The general findings of population synthesis are that neither channel, SD or DD, can produce the observed number of SNe Ia (Ruiter et al. 2009; Mennekens et al. 2010). Mennekens et al. (2010), using the Brussels population synthesis code, find that the morphological shape of the observed DTD cannot be fit by the SD scenario alone. Instead, a combination of both SD and DD scenarios will fit the morphological shape but produces approximately three times fewer SNe Ia than is observed. A similar study by Ruiter et al. (2009), using the population synthesis code `StarTrack`, also find that the combination of SD and DD scenarios fits the observed shape of DTD, but accounts for ten times fewer SNe Ia than observed. Population synthesis would then seem to indicate that neither scenario alone can produce the morphological shape of the DTD and that even the combination of both cannot produce the absolute number of observed SNe Ia.

#### 4. Line Identifications in Cools

We begin our analysis of CL SNe Ia by making line identifications. Identifying lines in SNe can be a difficult process and is further complicated in CLs due to the large number of ions with lower excitation temperatures and many metals which potentially are present as blends in the 4200 Å trough. Our sample contains spectra from SN 1991bg, SN 1997cn, SN 1999by, and SN 2005bl. We find the nine ions—O I, Na I, Mg II, Si II, S II, Ca II, Ti II, Cr II, and Fe II—of varying strengths and levels of stratification fit most of the observed spectral features well for all epochs considered with a tenth ion, Ca I, present in the early spectra.

All with respect to  $B$  maximum, we will make comparisons of five subsets of spectra from different epochs. In §4.1 we compare SN 1999by and SN 2005bl at day  $-3$ . The observed and synthetic spectra for this comparison are shown in Figure 4 and the fitting parameters are listed in Tables 1–2. In §4.2 we analyze the spectra of SN 1991bg, SN 1997cn, SN 1999by, and SN 2005bl just past  $B$  max. These spectra can be found in Figures 5–6 with fitting parameters listed in Tables 3–6. Synthetic spectra and line identifications for SN 1991bg at day 18 and SN 2005bl at day 19 are summarized in §4.3 and displayed in Figure 8 with fitting parameters listed in Tables 7–8. In §4.4, spectra from approximately one month post  $B$  maximum for SN 1991bg, SN 1997cn, and SN 1999by are discussed. The spectra at this epoch are plotted in Figures 9–10 with fitting parameters displayed in Tables 9–13. A great deal of spectroscopic analysis has been performed on SN 1991bg by Filippenko et al. (1992a); Leibundgut et al. (1993); Turatto et al. (1996); Mazzali et al. (1997) and Branch et al. (2006, 2008, 2009). Turatto et al. (1998) have analyzed SN 1997cn. Garnavich et al. (2004) and Höflich et al. (2002) considered SN 1999by. Taubenberger et al. (2008) and Hachinger et al. (2009) performed an analysis of SN 2005bl.

#### 4.1. Day 3 Pre $B$ Maximum Spectra

The day  $-3$  spectra are presented in Figure 4. The **SYNOW** spectra for SN 1999by and SN 2005bl are overplotted with their respective observed spectra, and spectral absorptions are labeled. The synthetic spectra parameters are given in Tables 1–2.

The broad absorption trough at  $4200 \text{ \AA}$ , characteristic of the CL subgroup, is well fit by a combination of Ti II and Mg II. This trough is continually fit by both Ti II and Mg II in all modeled spectra. Garnavich et al. (2004), while modeling SN 1999by with **SYNOW**, find the absorption at  $5000 \text{ \AA}$  to be fit by Mg I, whereas we attribute this feature to Ti II and find no need of Mg I. Both Ti II and Mg I have an absorption at about  $5000 \text{ \AA}$ ; however, **SYNOW** fits with Ti II and without Mg I give accurate fits for this absorption. Mg I, while possibly present, when included is not the main contributor to this feature and has no other absorptions or emissions which can clearly be attributed to it. Thus we consider the identification of Mg I to not be required. Ti II also contributes to the  $5780 \text{ \AA}$  feature. The  $7630 \text{ \AA}$  feature, blended into the O I triplet, belongs to Mg II. For these reasons Ti II and Mg II can be considered definite. Other definite ions include Si II, Ca II, Fe II, and O I which all contribute to multiple absorptions.

The other four ions, Ca I, Cr II, S II, and Na I, only contribute to one absorption each and, although quite likely, are not definite. The “W” feature at  $5330 \text{ \AA}$ , often attributed to S II, may also be fit by features due to Sc II; Branch et al. (2006) have indeed produced **SYNOW** fits with this attribution. Although synthetic fits with Sc II are possible, S II is more likely in the SNe Ia scenario, we discuss this further below. Na I creates a shoulder in the  $5650 \text{ \AA}$  emission, and although very weak in the early spectra, becomes much more conspicuous later. Based on the evolution of multiple epochs, even though Na I is weak early, it is highly likely to be present. Na I is a common identification of this feature in CL SNe Ia (Filippenko et al. 1992a; Garnavich et al. 2004; Taubenberger et al.

2008); however, Mazzali et al. (1997) when using W7 cannot reproduce this feature without adding extra Na I and modifying their abundance distributions, while Leibundgut et al. (1993) identify it as a blend of Si II. Ca I matches the absorption at 5980 Å in these spectra, but disappears sometime after day 4 post *B* max and before day 18. Garnavich et al. (2004) identifies two Ca I absorptions as late as day 7 in SN 1999by and Taubenberger et al. (2008) make no Ca I identifications for SN 2005bl. The remaining ion, Cr II, is found at the 4700 Å absorption and further helps to block the emission at 4600 Å, in agreement with Taubenberger et al. (2008), but unidentified by Garnavich et al. (2004).

Aside from Garnavich et al. (2004) identifying Mg I in SN 1999by at 5000 Å instead of Cr II, our other line identifications are in good agreement. An analysis performed by Hachinger et al. (2009) on SN 2005bl identifies small amounts (less than 10% of the mass fraction) of C II in agreement with Taubenberger et al. (2008) who also find C II. C II is possible, however does not add any benefits to our synthetic fits and as noted by Hachinger et al. (2009) is a break from other CL SNe Ia such as SN 1991bg and SN 1999by in which C II has not been identified. In fact, C II is more often associated with superluminous, rather than subluminous, SNe Ia (Howell et al. 2006; Hicken et al. 2007; Parrent et al. 2011).

#### 4.2. Days 2, 3, and 4 Post *B* Maximum Spectra

Figures 5–6 show the observed and synthetic spectra for SN 1991bg, SN 1997cn, SN 1999by and SN 2005bl at days 2, 3, 3, and 4, respectively. The spectrum for SN 1997cn ends at 7400 Å, which is before the O I feature and Mg II absorption at 7630 Å; however these ions are still used in the **SYNOW** fits as they contribute to the overall shape of the spectra. The fitting parameters used for these synthetic spectra are given in Tables 3–6.

As usual we consider Si II, Ca II, Fe II, and O I definitely present for their contribution to multiple spectral features. Also, Ti II and Mg II are definite ions except in the case of 1997cn where the Mg II feature at 7630 Å is not available to be modeled. Due to the attribution of Mg II to the absorption trough in SN 1997cn we still consider it highly likely. Again, Cr II continues to be present at 4700 Å and helps to reduce the emission just blueward of its absorption. We consider the presence of Cr II not only plausible but likely. Further, during these early spectra Ca I fits the absorption at 5980 Å.

In comparison with the analysis by Turatto et al. (1998) on SN 1997cn, we continue to see good agreement with the primary differences being Ca I and Cr II which they do not identify. Turatto et al. (1998) also identifies Ni II at 4067 Å, which is possible, but we find no benefit in the inclusion of Ni II in our fits.

Close examination of the fitting parameters given for these SNe in Tables 3–6 will show that both 1997cn and 2005bl have photospheric velocities ( $v_{phot}$ ) of 7,600 km s<sup>-1</sup> which is significantly lower than 1991bg at 11,000 km s<sup>-1</sup> and 1999by at 10,000 km s<sup>-1</sup>. Looking forward to days 18 and

19 we see that 2005bl has a lower gradient in  $v_{phot}$  than does 1991bg and differs by only  $100 \text{ km s}^{-1}$ . By days 28, and 29 the differences in  $v_{phot}$  between the SNe are insignificant.

Figure 7 compares the fit of SN 1999by at day +3, using S II and Sc II to fit the “W” feature usually attributed to S II. It is hard to definitively decide between the two fits and without the strong S II  $\lambda 6355$  line, the identification of SN 1999by as a SNe Ia becomes weaker. This effect is important but needs to be followed up in future work with more detailed spectral modeling.

### 4.3. Days 18 and 19 Post $B$ Maximum Spectra

All the same ions as discussed in §§4.1–4.2, except Ca I, are still present by days 18 and 19, but the spectra have several noticeable differences from the early time spectra. (Synthetic and observed spectra for SN 1991bg and SN 2005bl can be seen in Figure 8.) Primarily the differences include the ions having deeper absorptions, higher emissions, and lower  $v_{phot}$ . The most obvious difference is the Na I absorption at  $5700 \text{ \AA}$ , which is no longer just a shoulder in an emission but a rather strong and sharp absorption. We still find Si II, Ca II, Fe II, Ti II, Mg II, and O I definite whereas Na I is now much more likely. Cr II and S II are plausible for the same reasons as before and Ca I is no longer used in the synthetic spectra.

### 4.4. Days 28, 29, 31, and 32 Post $B$ Maximum Spectra

Figures 9–10 have the synthetic and observed spectra for SN 1991bg, SN 1997cn, and SN 1999by where the absorptions are well fit; however, in the red the synthetic emissions are weak. This lack of strong emissions can be explained by the assumptions of **SYNOW** itself. **SYNOW** assumes a perfect blackbody emitter and absorber with a sharp photosphere surrounded by a homologous and spherically expanding ion cloud where lines form by resonance scattering treated in the Sobolev approximation. These assumptions do not allow for net emission profiles. Once ions begin to enter net emission **SYNOW** can no longer reproduce the strong emission peaks well. To overcome this issue it is possible to increase greatly the optical depth and rescale, but better fits are often obtained simply by leaving these emissions alone and focusing on the absorptions.

The same nine ions are present in these spectra as the previous, but O I has been strongly stratified to fit the three separate absorptions at about  $7530 \text{ \AA}$ . Furthermore, a deep and wide absorption around  $6700 \text{ \AA}$  to  $7000 \text{ \AA}$  has appeared. Despite our best efforts we were unable to fit this trough in a reasonable way. We tried a variety of ions including C I and O II, which could fill some of the trough but not without heavy restriction in  $v_{min}$  and  $v_{max}$ . None of the attempts proved successful and we do not find any of these ions likely.



## 5. Intermediate Type Ia Supernovae

Figure 11 is another WW plot very similar to Figure 1, but in this WW plot, intermediates are included. Intermediates are SNe Ia that do not necessarily fall into any particular subgroup; instead they fall in between, sharing properties of the different subgroups. What we find when including the intermediates is that the subgroups begin to blend, indicating that rather than being discrete, SNe Ia subgroups, as delineated by Branch, are a continuous distribution based on multiple parameters. Branch et al. (2006, 2009) did extensive work on spectroscopic subclassification of SNe Ia and came to a similar conclusion.

Recent work of Maeda et al. (2010) indicates that some of the spectral diversity of SNe Ia is a result of the viewing angle on an asymmetrically exploding WD progenitor. Maeda et al. (2010) used the Benetti classification scheme of FAINT, HVG, and LVG. Using the emission lines Fe II  $\lambda 7155$  and Ni II  $\lambda 7378$  lines, which occur during the nebular phase, they measured the Doppler shift in the ejecta. Blue-shifted lines will be on the near side and red-shifted will be on the far side of an exploding SN. They found a diversity in the velocities of the blue-shifted and red-shifted lines implying that the initial SN ignition occurred off-center. Measurement of red-shift and blue-shift in HVG and LVG SNe Ia show that HVGs are preferentially red-shifted and LVGs blue-shifted. Maeda et al. (2010) conclude that LVGs are viewed in the direction of the initial spark and HVGs are viewed opposite the spark. Statistical treatment of this result indicates a high probability that the differences of the two groups is entirely an effect of viewing angle. The work of Maeda et al. (2010) explained why the differences between the HVG and LVG groups occurred, but did little to address the FAINT group which they acknowledge may arise from a completely different explosion mechanism than HVGs and LVGs.

## 6. Discussion

Due to the high level of importance placed on SNe Ia, a complete understanding of their physical nature is paramount. One method to probe this nature is examination of their differences. Thus, we analyzed the spectroscopically CL subgroup of SNe Ia. In summary, SNe in this subgroup are underluminous, rapid decliners, and poor  $^{56}\text{Ni}$  producers with deep and wide absorption troughs around  $4200 \text{ \AA}$  due to Ti II and unusually strong Si II  $\lambda 5972$  absorptions. The path leading to subluminous SNe Ia is presently uncertain. SD scenarios in which a delayed-detonation, where a subsonic deflagration front transitions into a detonation, are strong theoretically and account well for observations (Höfllich et al. 2010). There also exist competing DD scenarios such as that presented by Pakmor et al. (2011) which indicate SNe Ia potentially originate from the merger of two CO WDs. Each scenario has its own strengths and weaknesses and the question of progenitors remains open. Furthermore, population synthesis studies tell us that neither scenario alone can account for the total number of observed SNe Ia.

We have modeled the spectra of several CL SNe Ia with the fast and highly parameterized

synthetic spectrum code **SYNOW** and compared our findings with those of similar studies. We find good agreement with other studies. Our work indicates many ions are potentially present in CLs, and line identifications are complicated for this reason. We show that Si II, Ca II, Fe II, Ti II, Mg II and O I are the most definite ions present in the spectra of cools. It is also very likely that Na I is present. Three other ions, Ca I, Cr II, and S II, are considered as possibilities. S II is quite likely, but Ca I and Cr II only occur in one location in our synthetic spectra and they have not been definitively explained in other studies. Therefore we consider these ions possible but not definite.

Examining the velocity evolution of Si II  $\lambda 6355$  shows the primary difference among this subgroup. From our models we see that SN 2005bl and SN 1999by have lower Si II  $\lambda 6355$  velocities than SN 1991bg and SN 1997cn in early time spectra but have lower velocity gradients so that by about day 18 post  $B$  maximum all four CLs have approximately the same velocity. Si II  $\lambda 6355$  velocities are plotted in Figure 12 for several CLs and CNs. Comparing our velocities with those of other studies show insignificant differences. Overall, the appearance of the velocity distribution for all SNe Ia is quite continuous.

Our examination of this subgroup indicates that 1991bg-likes are fairly homogeneous amongst themselves (albeit somewhat due to construction) and not only share the same ions, but fitting parameters and properties as well. Upon consideration of intermediates the distinctions among the subgroups begin to blur even more and the distribution of SNe Ia seems increasingly continuous. With a large and well-observed sample this distribution may take a form similar to the hypothetical distribution displayed in Figure 13.

A continuous distribution of SNe Ia could have regions of high density and low density in the WW plots, but the difference in density should be fairly small. These dense regions would contain the subgroups. The highest density region would contain the most common SNe Ia, the CNs. The lowest density regions would contain SNe Ia which are steps away from one subgroup toward another; intermediates. The reason for different regions of high density and low density, i.e. the subgroups, could indicate sets of secondary parameters which are slightly more stable and thus more likely to be reproduced for WDs transitioning into SNe Ia, rather than fundamentally different processes.

Present work on the diversity of SNe Ia is incomplete but is leading to the conclusion that rather than being made of discrete subgroups, SNe Ia are a continuous distribution of the same phenomenon. However, for more definitive conclusions it is necessary to have a much larger and well-observed sample coupled with more robust explosion models.

## 7. Acknowledgments

We thank David Branch for many helpful discussions, Saurabh Jha for providing his data, and Stefano Benetti for providing his data. We thank the anonymous referee for improving our presentation and bringing the S II versus Sc II identification question into clearer focus.

This work was supported in part by NSF grant AST-0707704, US DOE Grant DE-FG02-07ER41517, and NASA Grant HST-GO-12298.05-A. Support for Program number HST-GO-12298.05-A was provided by NASA through a grant from the Space Telescope Science Institute, which is operated by the Association of Universities for Research in Astronomy, Incorporated, under NASA contract NAS5-26555.

## REFERENCES

- Arnett, W. D., Branch, D., & Wheeler, J. C. 1985, *Nature*, 314, 337
- Baade, W. 1938, *ApJ*, 88, 285
- Benetti, S. 2005, in *Astronomical Society of the Pacific Conference Series*, Vol. 342, 1604-2004: Supernovae as Cosmological Lighthouses, ed. M. Turatto, S. Benetti, L. Zampieri, & W. Shea, 235
- Benetti, S., Cappellaro, E., Mazzali, P. A., Turatto, M., Altavilla, G., Bufano, F., Elias-Rosa, N., Kotak, R., Pignata, G., Salvo, M., & Stanishev, V. 2005, *ApJ*, 623, 1011
- Branch, D., Benetti, S., Kasen, D., Baron, E., Jeffery, D. J., Hatano, K., Stathakis, R. A., Filippenko, A. V., Matheson, T., Pastorello, A., Altavilla, G., Cappellaro, E., Rizzi, L., Turatto, M., Li, W., Leonard, D. C., & Shields, J. C. 2002, *ApJ*, 566, 1005
- Branch, D., Dang, L. C., & Baron, E. 2009, *PASP*, 121, 238
- Branch, D., Dang, L. C., Hall, N., Ketchum, W., Melakayil, M., Parrent, J., Troxel, M. A., Casebeer, D., Jeffery, D. J., & Baron, E. 2006, *PASP*, 118, 560
- Branch, D., Garnavich, P., Matheson, T., Baron, E., Thomas, R. C., Hatano, K., Challis, P., Jha, S., & Kirshner, R. P. 2003, *AJ*, 126, 1489
- Branch, D., Jeffery, D. J., Parrent, J., Baron, E., Troxel, M. A., Stanishev, V., Keithley, M., Harrison, J., & Bruner, C. 2008, *PASP*, 120, 135
- Branch, D., Parrent, J., Troxel, M. A., Casebeer, D., Jeffery, D. J., Baron, E., Ketchum, W., & Hall, N. 2007, in *AIP Conference Series*, Vol. 924, *The Multicolored Landscape of Compact Objects and Their Explosive Origins*, ed. T. di Salvo, G. L. Israel, L. Piersant, L. Burderi, G. Matt, A. Tornambe, & M. T. Menna, 342–349
- Branch, D. & Tammann, G. A. 1992, *ARA&A*, 30, 359
- Chuang, C. & Wang, Y. 2011, *ArXiv e-prints*, astro-ph/1102.2251

- Conley, A., Guy, J., Sullivan, M., Regnault, N., Astier, P., Balland, C., Basa, S., Carlberg, R. G., Fouchez, D., Hardin, D., Hook, I. M., Howell, D. A., Pain, R., Palanque-Delabrouille, N., Perrett, K. M., Pritchett, C. J., Rich, J., Ruhlmann-Kleider, V., Balam, D., Baumont, S., Ellis, R. S., Fabbro, S., Fakhouri, H. K., Fourmanoit, N., González-Gaitán, S., Graham, M. L., Hudson, M. J., Hsiao, E., Kronborg, T., Lidman, C., Mourao, A. M., Neill, J. D., Perlmutter, S., Ripoche, P., Suzuki, N., & Walker, E. S. 2011, *ApJS*, 192, 1
- Copin, Y., Blanc, N., Bongard, S., Gangler, E., Saugé, L., Smadja, G., Antilogus, P., Garavini, G., Gilles, S., Pain, R., Aldering, G., Bailey, S., Lee, B. C., Loken, S., Nugent, P., Perlmutter, S., Scalzo, R., Thomas, R. C., Wang, L., Weaver, B. A., Pécontal, E., Kessler, R., Baltay, C., Rabinowitz, D., & Bauer, A. 2006, *New A Rev.*, 50, 436
- Filippenko, A. V., Richmond, M. W., Branch, D., Gaskell, M., Herbst, W., Ford, C. H., Treffers, R. R., Matheson, T., Ho, L. C., Dey, A., Sargent, W. L. W., Small, T. A., & van Breugel, W. J. M. 1992a, *AJ*, 104, 1543
- Filippenko, A. V., Richmond, M. W., Matheson, T., Shields, J. C., Burbidge, E. M., Cohen, R. D., Dickinson, M., Malkan, M. A., Nelson, B., Pietz, J., Schlegel, D., Schmeer, P., Spinrad, H., Steidel, C. C., Tran, H. D., & Wren, W. 1992b, *ApJ*, 384, L15
- Fisher, A. K. 2000, PhD thesis, THE UNIVERSITY OF OKLAHOMA, unpublished
- Garnavich, P. M., Bonanos, A. Z., Krisciunas, K., Jha, S., Kirshner, R. P., Schlegel, E. M., Challis, P., Macri, L. M., Hatano, K., Branch, D., Bothun, G. D., & Freedman, W. L. 2004, *ApJ*, 613, 1120
- Goobar, A., Perlmutter, S., Aldering, G., Goldhaber, G., Knop, R. A., Nugent, P., Castro, P. G., Deustua, S., Fabbro, S., Groom, D. E., Hook, I. M., Kim, A. G., Kim, M. Y., Lee, J. C., Nunes, N. J., Pain, R., Pennypacker, C. R., Quimby, R., Lidman, C., Ellis, R. S., Irwin, M., McMahon, R. G., Ruiz-Lapuente, P., Walton, N., Schaefer, B., Boyle, B. J., Filippenko, A. V., Matheson, T., Fruchter, A. S., Panagia, N., Newberg, H. J. M., & Couch, W. J. 2000, *Physica Scripta Volume T*, 85, 47
- Hachinger, S., Mazzali, P. A., Taubenberger, S., Pakmor, R., & Hillebrandt, W. 2009, *MNRAS*, 399, 1238
- Hicken, M., Garnavich, P. M., Prieto, J. L., Blondin, S., DePoy, D. L., Kirshner, R. P., & Parrent, J. 2007, *ApJ*, 669, L17
- Hicken, M., Wood-Vasey, W. M., Blondin, S., Challis, P., Jha, S., Kelly, P. L., Rest, A., & Kirshner, R. P. 2009, *ApJ*, 700, 1097
- Hillebrandt, W. & Niemeyer, J. C. 2000, *ARA&A*, 38, 191
- Hoefflich, P., Mueller, E., & Khokhlov, A. 1993, *A&A*, 268, 570

- Höflich, P. 2006, *Nuclear Physics A*, 777, 579
- Höflich, P., Gerardy, C. L., Fesen, R. A., & Sakai, S. 2002, *ApJ*, 568, 791
- Höflich, P., Krisciunas, K., Khokhlov, A. M., Baron, E., Folatelli, G., Hamuy, M., Phillips, M. M., Suntzeff, N., & Wang, L. 2010, *ApJ*, 710, 444
- Howell, D. A., Sullivan, M., Nugent, P. E., Ellis, R. S., Conley, A. J., Le Borgne, D., Carlberg, R. G., Guy, J., Balam, D., Basa, S., Fouchez, D., Hook, I. M., Hsiao, E. Y., Neill, J. D., Pain, R., Perrett, K. M., & Pritchett, C. J. 2006, *Nature*, 443, 308
- Iben, Jr., I. & Tutukov, A. V. 1984, *ApJS*, 54, 335
- Jeffery, D. J., Ketchum, W., Branch, D., Baron, E., Elmhamdi, A., & Danziger, I. J. 2007, *ApJS*, 171, 493
- Jha, S., Garnavich, P. M., Kirshner, R. P., Challis, P., Soderberg, A. M., Macri, L. M., Huchra, J. P., Barmby, P., Barton, E. J., Berlind, P., Brown, W. R., Caldwell, N., Calkins, M. L., Kannappan, S. J., Koranyi, D. M., Pahre, M. A., Rines, K. J., Stanek, K. Z., Stefanik, R. P., Szentgyorgyi, A. H., Väisänen, P., Wang, Z., Zajac, J. M., Riess, A. G., Filippenko, A. V., Li, W., Modjaz, M., Treffers, R. R., Hergenrother, C. W., Grebel, E. K., Seitzer, P., Jacoby, G. H., Benson, P. J., Rizvi, A., Marschall, L. A., Goldader, J. D., Beasley, M., Vacca, W. D., Leibundgut, B., Spyromilio, J., Schmidt, B. P., & Wood, P. R. 1999, *ApJS*, 125, 73
- Khokhlov, A. M. 1991, *A&A*, 245, 114
- Krisciunas, K. 2008, in *First Middle East-Africa, Regional IAU Meeting, held 5-10 April, 2008 in Cairo, Egypt*. Online at <http://www.mearim.cu.edu.eg/new/Proceeding.htm>, p.7
- Law, N. M., Kulkarni, S. R., Dekany, R. G., Ofek, E. O., Quimby, R. M., Nugent, P. E., Surace, J., Grillmair, C. C., Bloom, J. S., Kasliwal, M. M., Bildsten, L., Brown, T., Cenko, S. B., Ciardi, D., Croner, E., Djorgovski, S. G., van Eyken, J., Filippenko, A. V., Fox, D. B., Gal-Yam, A., Hale, D., Hamam, N., Helou, G., Henning, J., Howell, D. A., Jacobsen, J., Laher, R., Mattingly, S., McKenna, D., Pickles, A., Poznanski, D., Rahmer, G., Rau, A., Rosing, W., Shara, M., Smith, R., Starr, D., Sullivan, M., Velur, V., Walters, R., & Zolkower, J. 2009, *PASP*, 121, 1395
- Leibundgut, B., Kirshner, R. P., Phillips, M. M., Wells, L. A., Suntzeff, N. B., Hamuy, M., Schommer, R. A., Walker, A. R., Gonzalez, L., Ugarte, P., Williams, R. E., Williger, G., Gomez, M., Marzke, R., Schmidt, B. P., Whitney, B., Coldwell, N., Peters, J., Chaffee, F. H., Foltz, C. B., Rehner, D., Siciliano, L., Barnes, T. G., Cheng, K., Hintzen, P. M. N., Kim, Y., Maza, J., Parker, J. W., Porter, A. C., Schmidtke, P. C., & Sonneborn, G. 1993, *AJ*, 105, 301
- Li, W., Filippenko, A. V., Treffers, R. R., Riess, A. G., Hu, J., & Qiu, Y. 2001, *ApJ*, 546, 734

- Li, W., Leaman, J., Chornock, R., Filippenko, A. V., Poznanski, D., Ganeshalingam, M., Wang, X., Modjaz, M., Jha, S., Foley, R. J., & Smith, N. 2010, ArXiv e-prints
- LSST Science Collaborations, Abell, P. A., Allison, J., Anderson, S. F., Andrew, J. R., Angel, J. R. P., Armus, L., Arnett, D., Asztalos, S. J., Axelrod, T. S., & et al. 2009, ArXiv e-prints, astro-ph/0912.0201
- Maeda, K., Benetti, S., Stritzinger, M., Röpke, F. K., Folatelli, G., Sollerman, J., Taubenberger, S., Nomoto, K., Leloudas, G., Hamuy, M., Tanaka, M., Mazzali, P. A., & Elias-Rosa, N. 2010, *Nature*, 466, 82
- Maoz, D. & Badenes, C. 2010, *MNRAS*, 407, 1314
- Maoz, D., Mannucci, F., Li, W., Filippenko, A. V., Della Valle, M., & Panagia, N. 2011, *MNRAS*, 307
- Mazzali, P. A., Chugai, N., Turatto, M., Lucy, L. B., Danziger, I. J., Cappellaro, E., della Valle, M., & Benetti, S. 1997, *MNRAS*, 284, 151
- Mennekens, N., Vanbeveren, D., De Greve, J. P., & De Donder, E. 2010, *A&A*, 515, A89
- Nugent, P., Phillips, M., Baron, E., Branch, D., & Hauschildt, P. 1995, *ApJ*, 455, L147
- Pakmor, R., Hachinger, S., Röpke, F. K., & Hillebrandt, W. 2010, *Nature*, 463, 61
- . 2011, *A&A*, 528, A117
- Parkinson, D., Kunz, M., Liddle, A. R., Bassett, B. A., Nichol, R. C., & Vardanyan, M. 2010, *MNRAS*, 401, 2169
- Parrent, J. T., Thomas, R. C., Fesen, R. A., Marion, G. H., Challis, P., Garnavich, P. M., Milisavljevic, D., Vinkò, J., & Wheeler, J. C. 2011, ArXiv e-prints
- Pastorello, A., Mazzali, P. A., Pignata, G., Benetti, S., Cappellaro, E., Filippenko, A. V., Li, W., Meikle, W. P. S., Arkharov, A. A., Blanc, G., Bufano, F., Derekas, A., Dolci, M., Elias-Rosa, N., Foley, R. J., Ganeshalingam, M., Harutyunyan, A., Kiss, L. L., Kotak, R., Larionov, V. M., Lucey, J. R., Napoleone, N., Navasardyan, H., Patat, F., Rich, J., Ryder, S. D., Salvo, M., Schmidt, B. P., Stanishev, V., Székely, P., Taubenberger, S., Temporin, S., Turatto, M., & Hillebrandt, W. 2007, *MNRAS*, 377, 1531
- Patat, F., Benetti, S., Cappellaro, E., Danziger, I. J., della Valle, M., Mazzali, P. A., & Turatto, M. 1996, *MNRAS*, 278, 111
- Perlmutter, S., Aldering, G., Goldhaber, G., Knop, R. A., Nugent, P., Castro, P. G., Deustua, S., Fabbro, S., Goobar, A., Groom, D. E., Hook, I. M., Kim, A. G., Kim, M. Y., Lee, J. C., Nunes, N. J., Pain, R., Pennypacker, C. R., Quimby, R., Lidman, C., Ellis, R. S., Irwin,

- M., McMahon, R. G., Ruiz-Lapuente, P., Walton, N., Schaefer, B., Boyle, B. J., Filippenko, A. V., Matheson, T., Fruchter, A. S., Panagia, N., Newberg, H. J. M., Couch, W. J., & The Supernova Cosmology Project. 1999, *ApJ*, 517, 565
- Phillips, M. M. 1993, *ApJ*, 413, L105
- Riess, A. G., Filippenko, A. V., Challis, P., Clocchiatti, A., Diercks, A., Garnavich, P. M., Gilliland, R. L., Hogan, C. J., Jha, S., Kirshner, R. P., Leibundgut, B., Phillips, M. M., Reiss, D., Schmidt, B. P., Schommer, R. A., Smith, R. C., Spyromilio, J., Stubbs, C., Suntzeff, N. B., & Tonry, J. 1998, *AJ*, 116, 1009
- Riess, A. G., Macri, L., Casertano, S., Sosey, M., Lampeitl, H., Ferguson, H. C., Filippenko, A. V., Jha, S. W., Li, W., Chornock, R., & Sarkar, D. 2009, *ApJ*, 699, 539
- Ruiter, A. J., Belczynski, K., & Fryer, C. 2009, *ApJ*, 699, 2026
- Taubenberger, S., Hachinger, S., Pignata, G., Mazzali, P. A., Contreras, C., Valenti, S., Pastorello, A., Elias-Rosa, N., Bärnbantner, O., Barwig, H., Benetti, S., Dolci, M., Fliri, J., Folatelli, G., Freedman, W. L., Gonzalez, S., Hamuy, M., Krzeminski, W., Morrell, N., Navasardyan, H., Persson, S. E., Phillips, M. M., Rie, C., Roth, M., Suntzeff, N. B., Turatto, M., & Hillebrandt, W. 2008, *MNRAS*, 385, 75
- Timmes, F. X. & Woosley, S. E. 1992, *ApJ*, 396, 649
- Turatto, M., Benetti, S., Cappellaro, E., Danziger, I. J., Della Valle, M., Gouiffes, C., Mazzali, P. A., & Patat, F. 1996, *MNRAS*, 283, 1
- Turatto, M., Piemonte, A., Benetti, S., Cappellaro, E., Mazzali, P. A., Danziger, I. J., & Patat, F. 1998, *AJ*, 116, 2431
- Waagen, E., Evans, R. O., Villi, M., Cortini, G., Johnson, W., McNaught, R. H., Mueller, J., Cappellaro, E., Cutispoto, G., La Franca, F., Goldschmidt, C., Kirshner, R. P., & Peters, J. 1991, *IAU Circ.*, 5239, 1
- Webbink, R. F. 1984, *ApJ*, 277, 355
- Whelan, J. & Iben, Jr., I. 1973, *ApJ*, 186, 1007
- Wood-Vasey, W. M., Miknaitis, G., Stubbs, C. W., Jha, S., Riess, A. G., Garnavich, P. M., Kirshner, R. P., Aguilera, C., Becker, A. C., Blackman, J. W., Blondin, S., Challis, P., Clocchiatti, A., Conley, A., Covarrubias, R., Davis, T. M., Filippenko, A. V., Foley, R. J., Garg, A., Hicken, M., Krisciunas, K., Leibundgut, B., Li, W., Matheson, T., Miceli, A., Narayan, G., Pignata, G., Prieto, J. L., Rest, A., Salvo, M. E., Schmidt, B. P., Smith, R. C., Sollerman, J., Spyromilio, J., Tonry, J. L., Suntzeff, N. B., & Zenteno, A. 2007, *ApJ*, 666, 694





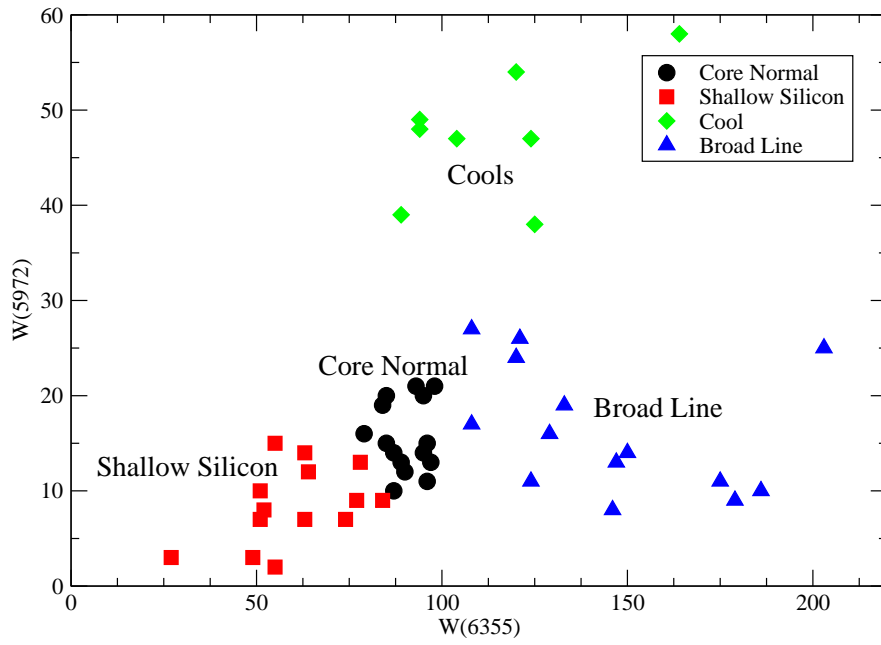


Fig. 1.— Pseudo-Equivalent Widths of  $\lambda 5972$  vs.  $\lambda 6355$ . Data comes from Branch et al. (2009) as well as private communication with D. Branch.

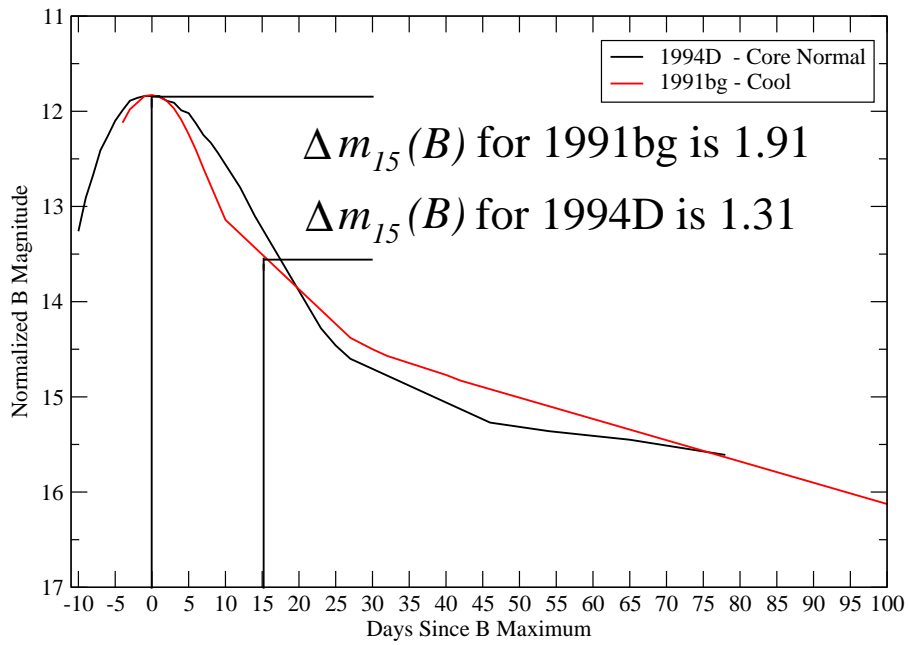


Fig. 2.— CN vs. CL Decline Rate Comparisons.  $\Delta m_{15}$  values originate from Pastorello et al. (2007), light curve data for 1991bg comes from Turatto et al. (1996), and light curve data for 1994D comes from Patat et al. (1996).

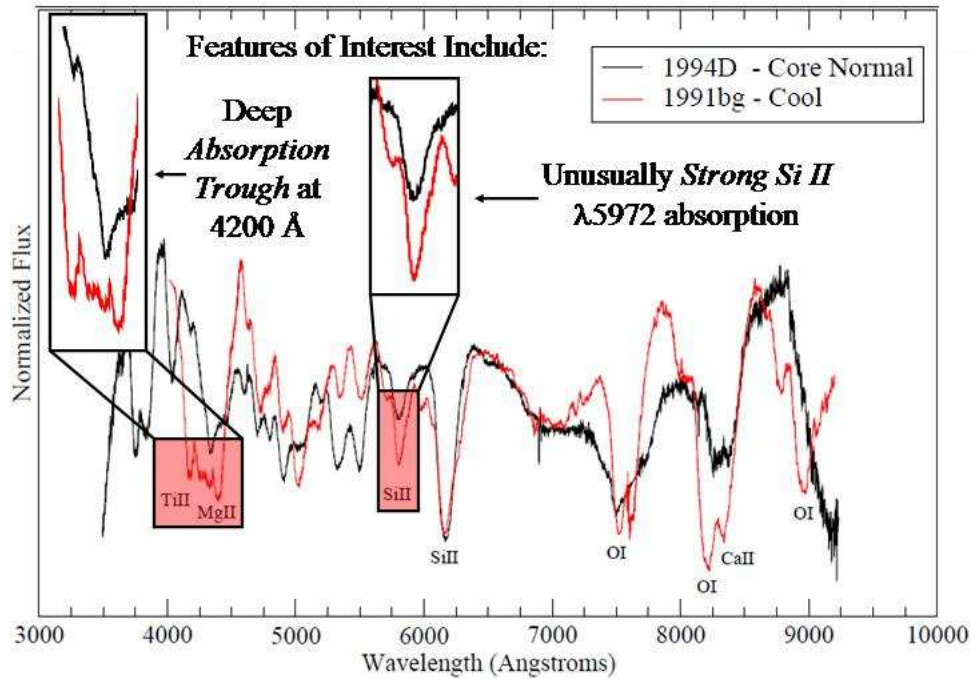


Fig. 3.— CN vs. CL Spectra Comparisons

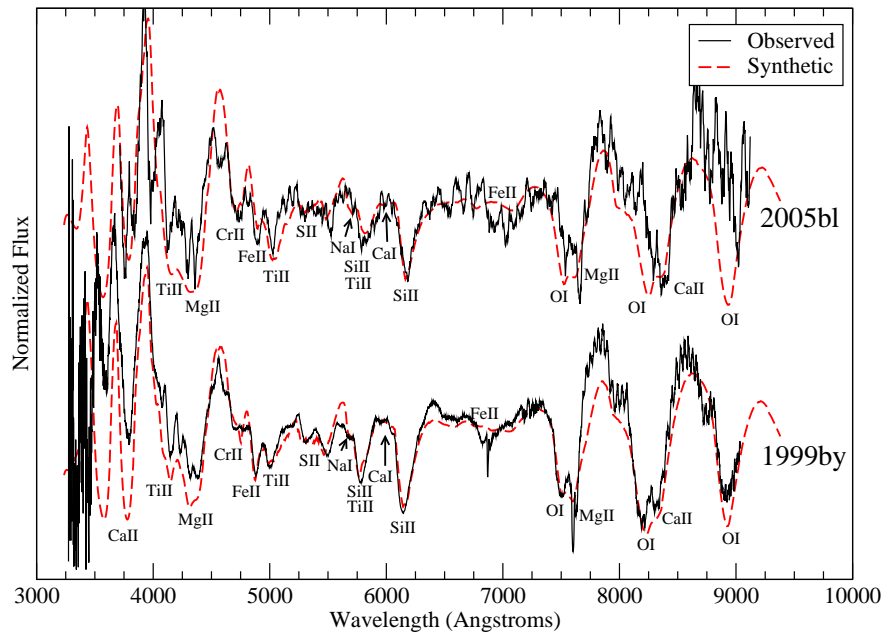


Fig. 4.— 2005bl and 1999by Day 3 Pre *B* Maximum. The telluric oxygen feature at 7594 Å is not marked.

Table 1. Fitting Parameters for 1999by Day 3 Pre  $B$  Maximum.

Element	$\tau$	$T_{exc}$ (K)	$v_{phot}$	$v_e$	$v_{min}$	$v_{max}$
HV <sub>e</sub> O I	4.5	7000	11	1.1	0	40
O I	-	-	-	-	-	-
Na I	1.1	7000	11	0.5	12.5	15
Mg II	20	7000	11	1.0	0	40
Si II	550	7000	11	0.5	0	13.5
S II	12	7000	11	0.2	0	40
Ca I	8.0	7000	10	1.0	0	40
Ca II	800	7000	11	1.2	0	40
Ti II	2	7000	11	2.0	0	40
Cr II	600	7000	11	1.0	0	40
Fe II	3.0	5000	11	1.0	0	40

\*All velocities are given in 1000 km s<sup>-1</sup>

Table 2. Fitting Parameters for 2005bl Day 3 Pre  $B$  Maximum.

Element	$\tau$	$T_{exc}$ (K)	$v_{phot}$	$v_e$	$v_{min}$	$v_{max}$
HV <sub>e</sub> O I	4.5	7000	10	1.4	0	40
O I	-	-	-	-	-	-
Na I	0.9	7000	10	0.5	12.5	14.5
Mg II	40	7000	10	1.0	0	40
Si II	80	7000	10	0.5	0	40
S II	8.0	7000	10	0.2	0	40
Ca I	8.0	7000	10	1.0	0	40
Ca II	1000	7000	10	1.0	0	40
Ti II	6.0	7000	10	2.0	0	40
Cr II	1200	7000	10	1.0	0	40
Fe II	3.0	7000	10	1.0	0	40

\*All velocities are given in 1000 km s<sup>-1</sup>

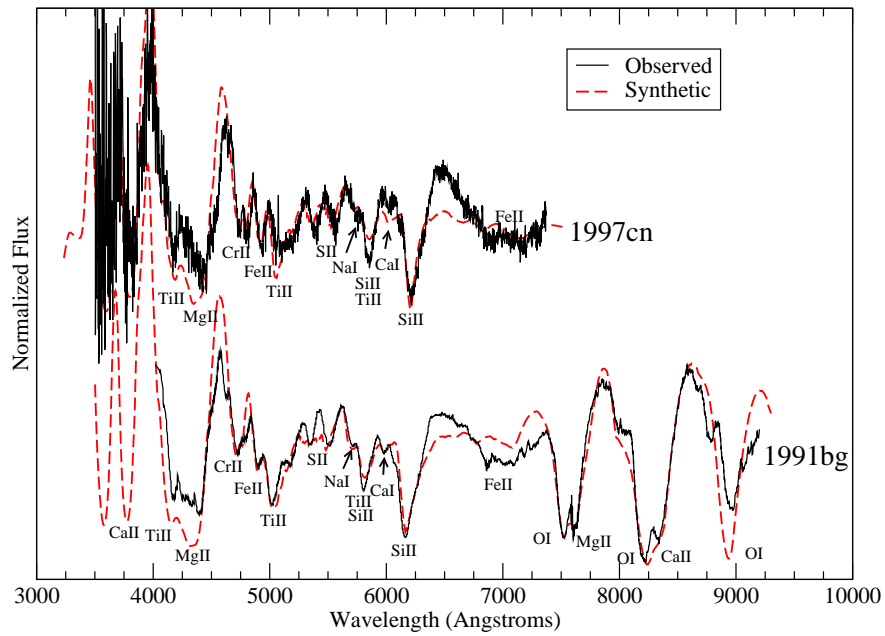


Fig. 5.— 1997cn Day 3 Post *B* Maximum and 1991bg Day 2 Post *B* Maximum. The telluric oxygen feature at 7594 Å is not marked.

Table 3. Fitting Parameters for 1991bg Day 2 Post  $B$  Maximum.

Element	$\tau$	$T_{exc}$ (K)	$v_{phot}$	$v_e$	$v_{min}$	$v_{max}$
HV <sub>e</sub> O I	5.0	7000	10	1.4	0	40
O I	-	-	-	-	-	-
Na I	0.5	7000	10	1.0	12.5	13.5
Mg II	40.0	7000	10	1.0	0	40
Si II	100	7000	10	0.5	0	40
S II	5.0	7000	10	0.2	0	40
Ca I	15.0	7000	10	1.0	0	40
Ca II	1100	7000	10	1.3	0	40
Ti II	6.0	7000	10	2.0	0	40
Cr II	1500	7000	10	1.0	0	40
Fe II	4.0	7000	10	1.0	0	40

\*All velocities are given in 1000 km s<sup>-1</sup>

Table 4. Fitting Parameters for 1997cn Day 3 Post  $B$  Maximum.

Element	$\tau$	$T_{exc}$ (K)	$v_{phot}$	$v_e$	$v_{min}$	$v_{max}$
HV <sub>e</sub> O I	5.0	7000	7.6	1.4	0	40
O I	-	-	-	-	-	-
Na I	0.1	7000	7.6	1.0	10.5	17.5
Mg II	40.0	7000	7.6	1.0	0	40
Si II	30.0	7000	7.6	0.6	0	40
S II	5.0	7000	7.6	0.2	0	40
Ca I	8.0	7000	10	1.0	0	40
Ca II	1100	7000	7.6	1.3	0	40
Ti II	4.0	7000	7.6	2.0	0	40
Cr II	1000	7000	7.6	1.0	0	40
Fe II	6.0	7000	7.6	1.0	0	40

\*All velocities are given in 1000 km s<sup>-1</sup>

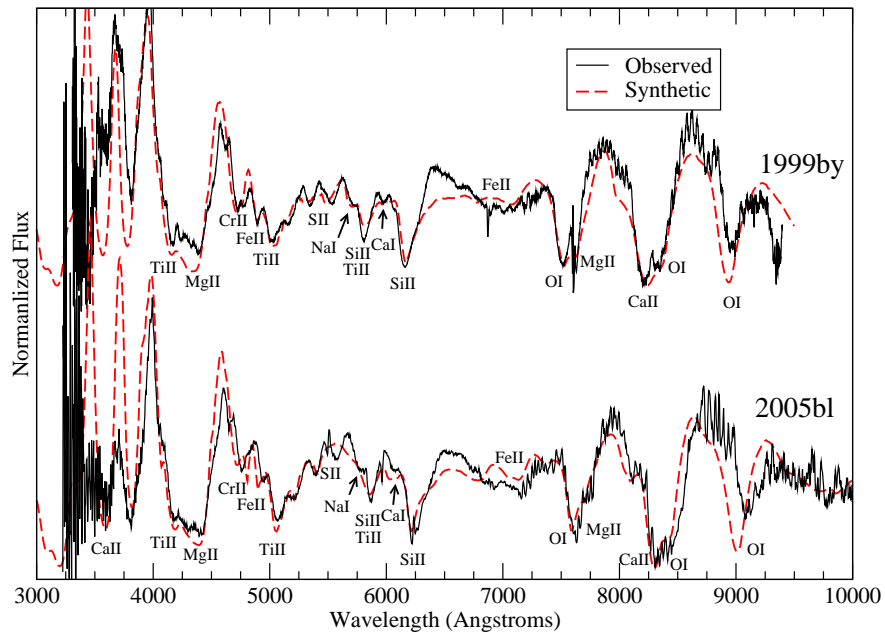


Fig. 6.— 1999by Day 3 Post *B* Maximum and 2005bl Day 4 Post *B* Maximum. The telluric oxygen feature at 7594 Å is not marked.



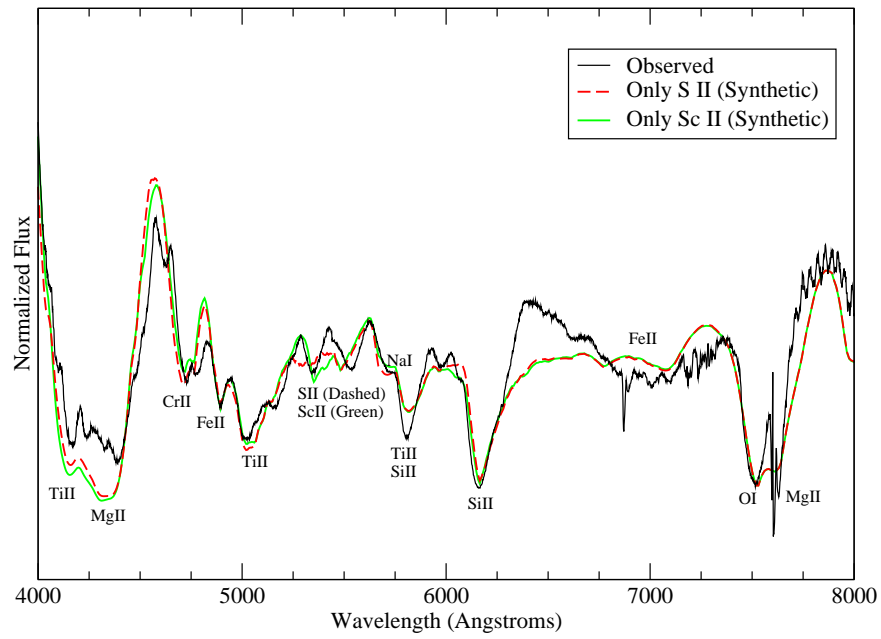


Fig. 7.— 1999by Day 3 Post *B* Maximum with the feature usually attributed to S II fit with both S II and Sc II. The telluric oxygen feature at 7594 Å is not marked.

Table 5. Fitting Parameters for 1999by Day 3 Post  $B$  Maximum.

Element	$\tau$	$T_{exc}$ (K)	$v_{phot}$	$v_e$	$v_{min}$	$v_{max}$
HV <sub>e</sub> O I	5.0	7000	10	1.4	0	40
O I	-	-	-	-	-	-
Na I	0.5	7000	10	1.0	12.5	13.5
Mg II	40.0	7000	10	1.0	0	40
Si II	100	7000	10	0.5	0	40
S II	5.0	7000	10	0.2	0	40
Ca I	12.0	7000	10	1.0	0	40
Ca II	1100	7000	10	1.3	0	40
Ti II	6.0	7000	10	2.0	0	40
Cr II	1500	7000	10	1.0	0	40
Fe II	4.0	7000	10	1.0	0	40

\*All velocities are given in  $1000 \text{ km s}^{-1}$

Table 6. Fitting Parameters for 2005bl Day 4 Post  $B$  Maximum.

Element	$\tau$	$T_{exc}$ (K)	$v_{phot}$	$v_e$	$v_{min}$	$v_{max}$
HV <sub>e</sub> O I	-	-	-	-	-	-
O I	4.5	7000	7.6	1.0	0	40
Na I	0.1	7000	7.6	1.0	10	12
Mg II	10.0	7000	7.6	1.0	0	40
Si II	10.0	7000	7.6	0.6	0	40
S II	1.0	7000	7.6	0.2	0	40
Ca I	8.0	7000	10	1.0	0	40
Ca II	800	7000	7.6	1.3	0	40
Ti II	7.0	7000	7.6	2.0	0	40
Cr II	600	7000	7.6	1.0	0	40
Fe II	6.0	7000	7.6	1.0	0	40

\*All velocities are given in  $1000 \text{ km s}^{-1}$

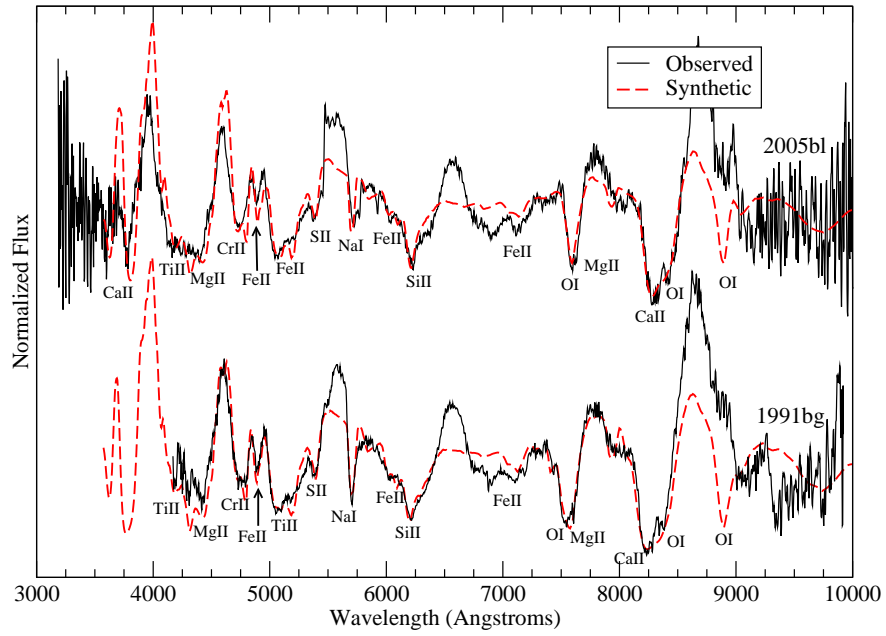


Fig. 8.— 2005bl Day 19 Post *B* Maximum, and 1991bg Day 18 Post *B* Maximum.

Table 7. Fitting Parameters for 1991bg Day 18 Post  $B$  Maximum.

Element	$\tau$	$T_{exc}$ (K)	$v_{phot}$	$v_e$	$v_{min}$	$v_{max}$
HV <sub>e</sub> O I	2.0	7000	8	1.6	0	40
O I	0.7	7000	8	1.0	15.2	16
Na I	9.0	7000	8	0.5	11	12
Mg II	3.5	7000	8	1.0	12	40
Si II	50	7000	8	0.5	0	40
S II	0.8	7000	8	1.0	14.5	40
Ca II	4000	7000	8	1.3	0	40
Ti II	12	7000	8	1.0	0	40
Cr II	2500	7000	8	1.0	0	40
Fe II	70	7000	8	0.7	0	40

\*All velocities are given in  $1000 \text{ km s}^{-1}$

Table 8. Fitting Parameters for 2005bl Day 19 Post  $B$  Maximum.

Element	$\tau$	$T_{exc}$ (K)	$v_{phot}$	$v_e$	$v_{min}$	$v_{max}$
HV <sub>e</sub> O I	1.0	7000	7.5	1.6	0	40
O I	-	-	-	-	-	-
Na I	3.0	7000	7.5	0.5	11	12
Mg II	2.0	7000	7.5	1.0	12	40
Si II	40	7000	7.5	0.5	0	40
S II	0.7	7000	7.5	1.0	14.5	40
Ca II	4000	7000	7.5	1.0	0	40
Ti II	17	7000	7.5	1.0	0	40
Cr II	2800	7000	7.5	1.0	0	40
Fe II	30	7000	7.5	0.8	0	40

\*All velocities are given in  $1000 \text{ km s}^{-1}$

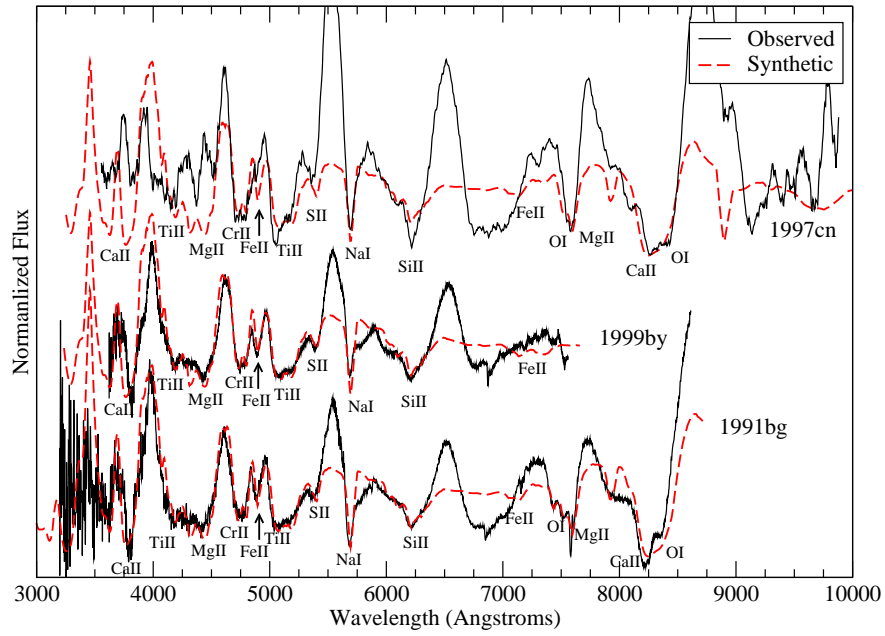


Fig. 9.— 1997cn Day 28 Post *B* Maximum, 1999by Day 29 Post *B* Maximum, and 1991bg Day 29 Post *B* Maximum.

Table 9. Fitting Parameters for 1997cn Day 28 Post  $B$  Maximum.

Element	$\tau$	$T_{exc}$ (K)	$v_{phot}$	$v_e$	$v_{min}$	$v_{max}$
HV <sub>e</sub> O I	0.6	7000	7.4	1.6	0	40
O I	0.4	7000	7.4	1.0	14	16
Na I	6.0	7000	7.4	0.7	11	40
Mg II	7.0	7000	7.4	1.0	12	13
Si II	10	7000	7.4	0.5	0	40
S II	0.4	7000	7.4	1.0	14	40
Ca II	4000	7000	7.4	1.3	0	40
Ti II	8.0	7000	7.4	1.0	0	40
Cr II	3000	7000	7.4	1.0	0	40
Fe II	50	7000	7.4	0.6	0	40

\*All velocities are given in 1000 km s<sup>-1</sup>

Table 10. Fitting Parameters for 1991bg Day 29 Post  $B$  Maximum.

Element	$\tau$	$T_{exc}$ (K)	$v_{phot}$	$v_e$	$v_{min}$	$v_{max}$
HV <sub>e</sub> O I	0.6	7000	7.6	1.6	0	40
O I	0.4	7000	7.6	1.0	14	16
Na I	6.0	7000	7.6	0.7	11	40
Mg II	7.0	7000	7.6	1.0	12	13
Si II	10	7000	7.6	0.5	0	40
S II	0.4	7000	7.6	1.0	14	40
Ca II	4000	7000	7.6	1.3	0	40
Ti II	8.0	7000	7.6	1.0	0	40
Cr II	3000	7000	7.6	1.0	0	40
Fe II	50	7000	7.6	0.6	0	40

\*All velocities are given in 1000 km s<sup>-1</sup>

Table 11. Fitting Parameters for 1999by Day 29 Post  $B$  Maximum.

Element	$\tau$	$T_{exc}$ (K)	$v_{phot}$	$v_e$	$v_{min}$	$v_{max}$
HV <sub>e</sub> O I	0.6	7000	7.6	1.6	0	40
O I	0.4	7000	7.6	1.0	14	16
Na I	3.0	7000	7.6	0.7	11	40
Mg II	7.0	7000	7.6	1.0	12	13
Si II	15	7000	7.6	0.5	0	40
S II	0.4	7000	7.6	1.0	14	40
Ca II	4000	7000	7.6	1.3	0	40
Ti II	8.0	7000	7.6	1.0	0	40
Cr II	3000	7000	7.6	1.0	0	40
Fe II	50	7000	7.6	0.6	0	40

\*All velocities are given in 1000 km s<sup>-1</sup>

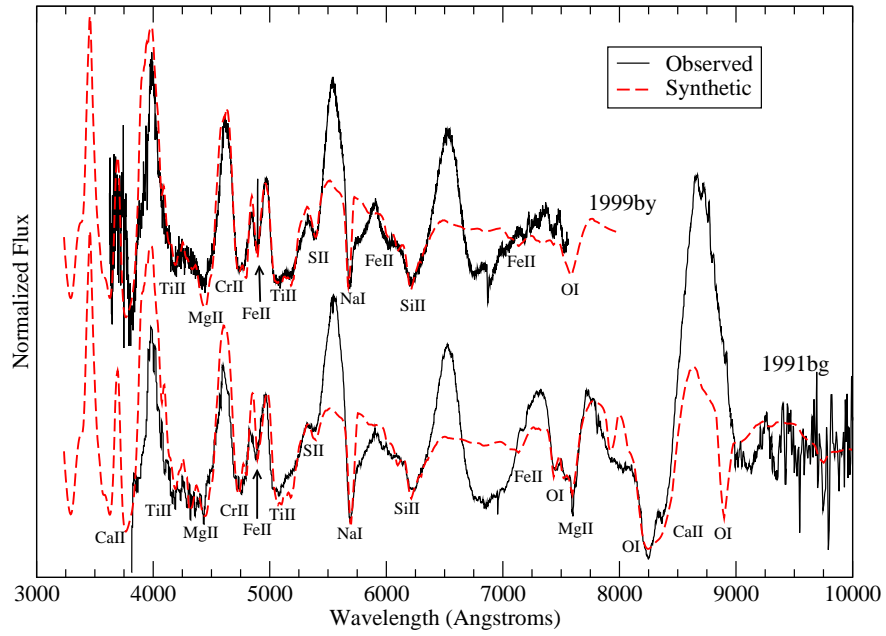


Fig. 10.— 1999by Day 31 Post *B* Maximum and 1991bg Day 32 Pre *B* Maximum.

Table 12. Fitting Parameters for 1999by Day 31 Post  $B$  Maximum.

Element	$\tau$	$T_{exc}$ (K)	$v_{phot}$	$v_e$	$v_{min}$	$v_{max}$
HV <sub>e</sub> O I	0.6	7000	7.5	1.6	0	40
O I	0.1	7000	7.5	1.0	0	40
Na I	3.5	7000	7.5	0.6	12	40
Mg II	0.1	7000	7.5	1.0	12	13
Si II	10	7000	7.5	0.6	0	40
S II	0.4	7000	7.5	1.0	14.5	40
Ca II	4000	7000	7.5	1.3	0	40
Ti II	7.0	7000	7.5	1.0	0	40
Cr II	3300	7000	7.5	1.0	0	40
Fe II	35	7000	7.5	0.8	0	40

\*All velocities are given in  $1000 \text{ km s}^{-1}$

Table 13. Fitting Parameters for 1991bg Day 32 Post  $B$  Maximum.

Element	$\tau$	$T_{exc}$ (K)	$v_{phot}$	$v_e$	$v_{min}$	$v_{max}$
HV <sub>e</sub> O I	0.6	7000	7.6	1.6	0	40
O I	0.5	7000	7.6	1.0	14	16
Na I	6.0	7000	7.6	0.6	11	40
Mg II	4.0	7000	7.6	1.0	12	14
Si II	10	7000	7.6	0.5	0	40
S II	0.1	7000	7.6	1.0	14.5	40
Ca II	4000	7000	7.6	1.3	0	40
Ti II	7.0	7000	7.6	1.0	0	40
Cr II	3500	7000	7.6	1.0	0	40
Fe II	40	7000	7.6	0.6	0	40

\*All velocities are given in  $1000 \text{ km s}^{-1}$



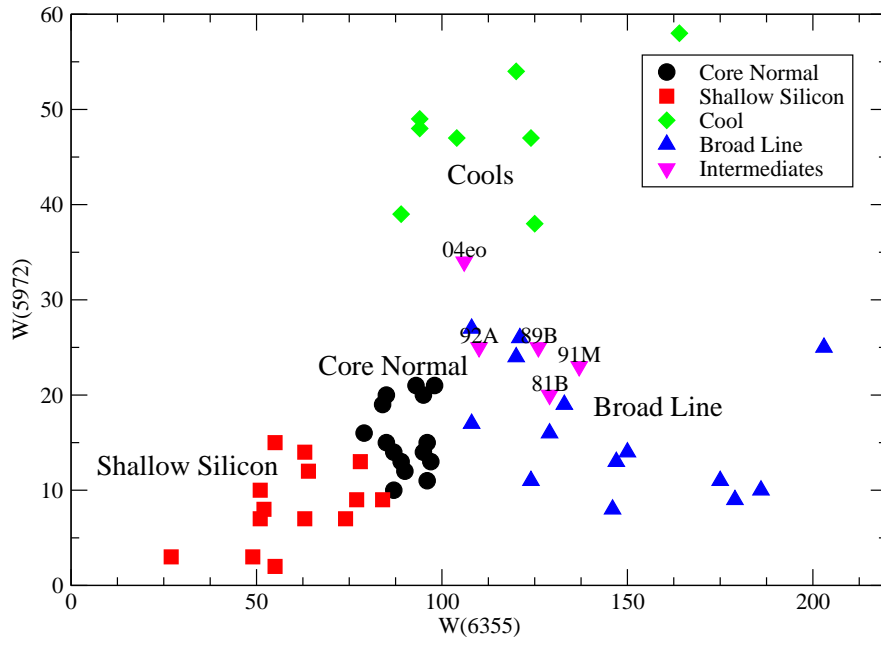


Fig. 11.— Pseudo-Equivalent Widths of  $\lambda 5972$  vs.  $\lambda 6355$  including intermediates. Data comes from Branch et al. (2009) as well as private communication with D. Branch.

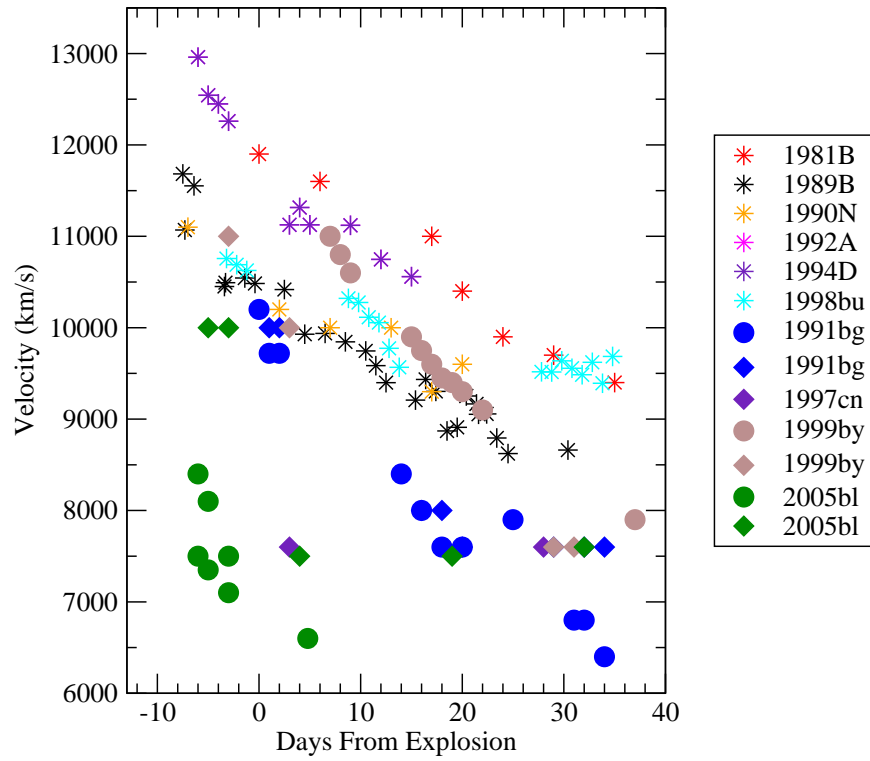


Fig. 12.— Si II  $\lambda 6355$  velocities. Filled symbols are CL SNe Ia and diamond symbols represent velocities from our data. Other line velocity data comes from Turatto et al. (1996); Jha et al. (1999); Garnavich et al. (2004) and Taubenberger et al. (2008).

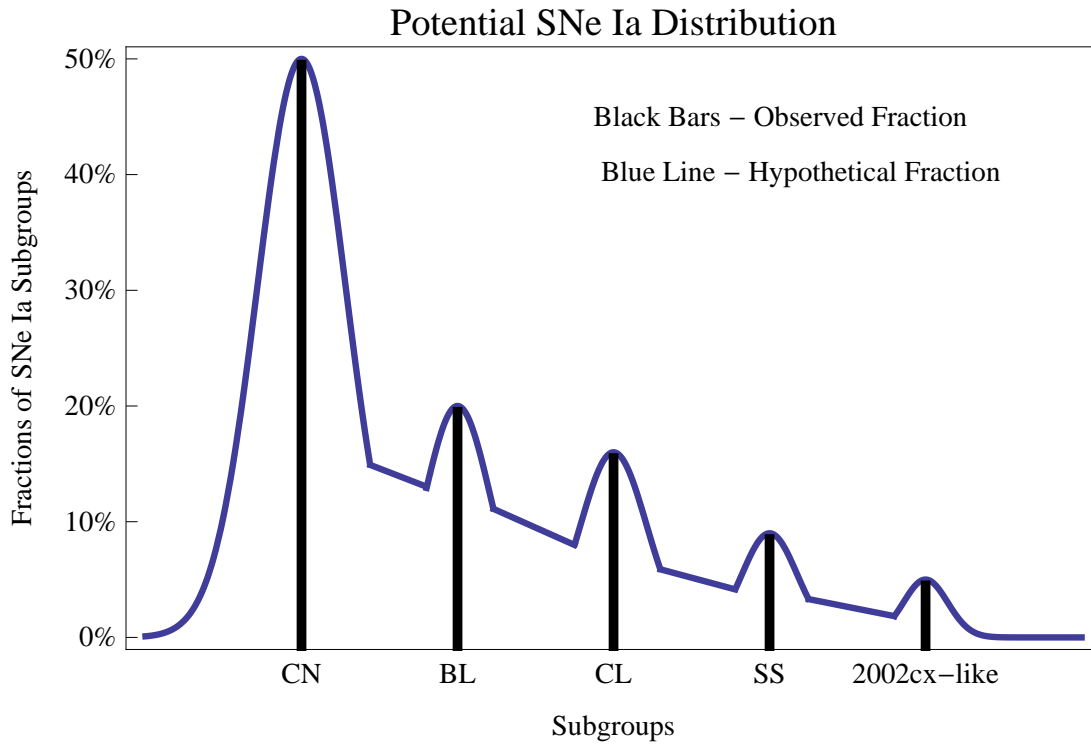


Fig. 13.— Cartoon SNe Ia distribution. The observed subgroup fraction data comes from Li et al. (2010).